Toward controlled geometric structure and surface property heterogeneities of TiO_2 for lipase immobilization

Wenfeng Zhou[a], Xiaohong Zhou[c], Wei Zhuang[a, d, *], Rijia Lin[e], Ye Zhao[b], Lei Ge[e,f, *], Ming Li[a], Jinglan Wu[a], Pengpeng Yang[a], Hongman Zhang[c], Chenjie Zhu[a, d, *], Hanjie Ying[a, d]

[a]State Key Laboratory of Materials-Oriented Chemical Engineering, College of Biotechnology and Pharmaceutical Engineering, National Engineering Technique Research Center for Biotechnology, Nanjing Tech University, No. 30, Puzhu South Road, Nanjing 211816, China

[b]School of Chemical Engineering, Zhengzhou University, Zhengzhou 450001, China

[c] School of Chemistry and Molecular Engineering, Nanjing Tech University, No. 30, Puzhu South Road, Nanjing 211816, China

[d]Synergetic Innovation Center for Advanced Materials, Nanjing Tech University, No. 30, Puzhu South Road, Nanjing 211816, China

[e]School of Chemical Engineering, The University of Queensland, St Lucia, Queensland 4072, Australia

[f]Centre for Future Materials, University of Southern Queensland, Springfield Central, QLD 4300, Australia.

*To whom correspondence should be addressed.

Contact information:

Dr. Wei Zhuang, Email: weizhuang@njtech.edu.cn

Dr. Lei Ge, Email: lei.ge@usq.edu.au

Dr. Chenjie Zhu, Email: zhucj@njtech.edu.cn

ABSTRACT

Immobilized enzymes as biocatalysts are expected to solve issues of pollution and economic inefficiency in industrial catalysis. In order to obtain an immobilized enzyme with high activity and stability, the design of substrate geometric structure and surface properties is desirable. Here, TiO_2 with controlled pore size and surface properties was designed and synthesized for lipase immobilization, resulting in an efficient biocatalyst. The activity of TiO_2 immobilized lipase is improved with the increasing pore size of TiO_2 from 10 to 100 nm. Compared to geometric structure impact, regulation of surface properties plays a greater role on the immobilization of lipase on TiO_2. Among them, the relative activity of ethenyl triethoxy silane (ETS) modified TiO_2 immobilized lipase is as high as 365.85 % over the pristine lipase. This research provides experimental evidence for studying the adsorption of enzyme molecules on the supports under the synergistic effect of geometric structure and surface properties.

Keywords: Heterogeneities, Geometric structure, Titanium dioxide, Coupling agents, Lipase immobilization

1. INTRODUCTION

Biocatalysis technology is one of the most promising technologies for industrial sustainable development. Immobilized enzyme as one of the most important biocatalysts has many advantages such as mildness, environmentally sustainable, high product purity and recoverability.[1] The selection of the support is fundamentally important to improve the stability of the enzyme by immobilization.[2] The properties of the support, including pore structure, topography, chemical composition, surface charge, and hydrophilicity/hydrophobicity, affect the structure and performance of the enzyme molecule.[3] Research of Pandya and co-workers[4] showed α-amylase cannot enter the pores of mesoporous silica such as MCM-41 and SBA-15 during the immobilization process. The resulting immobilized α-amylase has lower activity in catalytic starch conversion. In MCF-153 and MCF-335 with larger pore sizes, enzyme molecules are observed to enter the pores and have improved catalytic activity and stability.[4] Horseradish peroxidase (HRP) and oxalate oxidase (OxOx) immobilized on the support with stronger hydrophobicity have higher enzyme loading, stability and activity.[5]

Lipase (EC 3.1.1.3), an enzyme with multiple catalytic capabilities, is widely used in industry, such as oil processing, food, cosmetics, bioenergy, feed and others. Lipase can exert its maximum activity at the water-oil interface due to the α-helix structure lid.[8] Inside the lid is the catalytic site formed with the triplet structure (Ser-His-Asp).[9] Induced by the hydrophobicity of the oil phase, the lid is opened, and the substrate can access the catalytic site more easily.[10] It is the interfacial activation that greatly improves its catalytic performance such as the physical adsorption of lipase on the hydrophobic surface of the support. Compared with non-porous materials, porous materials are more beneficial to the stability of immobilized enzymes. A study from Gao *et al*.[11] exhibits the SBA-15 with a pore size of 15.6 nm is more suitable than that with the pore sizes of 6.8 nm, 9.1 nm, 13.2 nm and 22.4 nm as a support for lipase immobilization. Pore size greatly affects the adsorption of the enzyme. The ideal pore

size is 3-5 times of the size of the enzyme molecule. Generally, porous materials with the pores range from 10 to 100 nm are beneficial to improving the enzyme stability, and hydrophobic materials are good for increasing the catalytic activity of lipase.

Titanium dioxide (TiO_2) has high surface area, controllable pore size, abundant hydroxyl groups, non-toxic, antibacterial, and high biocompatibility. It has been used in cosmetics, coatings, semiconductors and other industrial fields.[12] TiO_2 has been regarded as potential support for enzyme immobilization.[13] TiO_2 was also be used as active particles to achieve *in situ* product/catalyst separation and catalyst recovery with the catalyst activity greater than 78 % after 10 times of use.[14] Laccase immobilized on TiO_2 can realize the high enzyme activity retained up to 88%, and the improved pH stability.[15]

The pore size of TiO_2 can be regulated in the range from 10 to100 nm by controlling the structure of the precursor and the calcination process.[16] The pore structure has a great effect on the enzyme loading and catalytic activity of the immobilized enzyme. According to the requirements of enzyme immobilization on the geometric structure of the material, the pore size of TiO_2 is designed. Only when the pore size matches the size of the enzyme molecule can higher activity and stability be obtained[17]. Within a suitable pore size range, the loading of enzyme molecules is usually proportional to the surface area of the support.[17] If the pore size is too small, the enzyme molecules will be blocked at the pore mouth and cannot enter the pore; if the pore size is too large, the enzyme molecules will easily escape from the support.[20] However, TiO_2 with a large number of hydroxyl groups on the surface is extremely hydrophilic, so it is not suitable for the immobilization of enzymes such as lipase. An excessively hydrophilic surface is likely to cause the blockage of lipase's active center and the reduction of enzyme activity. Zhou *et al.*[21] modified PMOs with different functional groups, such as ethylene and benzene, to change its surface properties. The results show that the hydrophobically functionalized PMOs-immobilized lipase has higher hydrolytic activity, a great improvement in the activity and stability. The hydrophobic modification on the supports' surface is beneficial to the catalytic activity of lipase

due to the interfacial activation of lipase. Commonly used reagents for modifying TiO_2 include salicylic acid, glutaraldehyde, silane coupling agent[22], and polylysine[13]. By grafting different functional groups on TiO_2, the catalytic activity of the immobilized enzyme is improved.[23] The research of Wu *et al.*[24] showed that TiO_2 modified by ε-Poly-L-lysine is more suitable for the immobilizing negatively charged enzymes and increasing operational stability, storage stability, thermal stability and reusability. In addition, the amino-terminal coupling agents can neutralize the negative charge on the surface of TiO_2, which is more suitable for the adsorption of negatively charged lipase than positive charge surface.

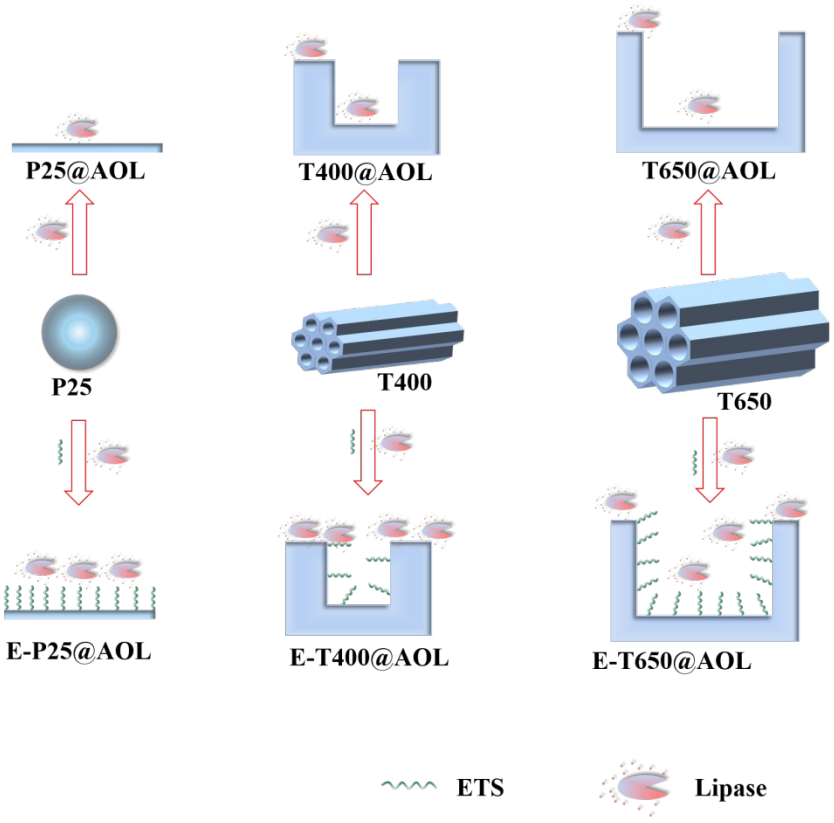

SCHEME 1 Mechanism diagram of the immobilization of AOL on pristine TiO_2 with different pore sizes or modified TiO_2 with ethenyl triethoxy silane (ETS).

Here, TiO_2 is used as the support for lipase immobilization. TiO_2 with different pore size are synthesized to study the effect of pore size on lipase immobilization. As indicated in Scheme 1, different coupling agents are used for hydrophobic modification and charge control of TiO_2 to improve the catalytic activity of lipase. In

addition, the effect of coupling agent modification and pore structure superimposition on the performance of lipase has also been studied. The effects of coupling agent modification and pore structure on the performance of immobilized enzymes were also compared and analyzed. Comparison and analysis are done to study the influence of coupling agents modification on pore size. Taking ethenyl triethoxy silane (ETS) as an example, Scheme1 shows the changes in pore structure and enzyme loading after ETS modified TiO_2. At the end, an immobilized enzyme with better performances is obtained. This process can provide the guidance for support selection and regulation in the future.

2. EXPERIMENTAL

2.1. Materials

Hydrated titanium dioxide($TiO_2 \cdot nH_2O$) was donated by Xiaohua Lu's Laboratory of Nanjing Tech University. P25 TiO_2 (P25), (3-Aminopropyl)-triethoxy silane (APTES), ethenyl triethoxy silane (ETS), 3-isocyanato propyl triethoxy silane (IPTS) and titanium tri-isostearoylisopropoxide (TTS) were purchased from Sigma-Aldrich (USA). Coomassie brilliant blue G-250, lipase from *Aspergillus oryzae* (AOL, ≥100,000 U/g), p-nitrophenyl palmitate (pNPP) and pnitrophenol (pNP) were purchased from Aladdin Reagent (Shanghai, China). Ethanol was purchased from Yasheng Chemical Co., Ltd. (Wuxi, China). Toluene, acetone were supplied by the Merck & Co Inc. Bovine serum albumin (BSA, =98%) was purchased from Shanghai Jinsui Bio-Technology Co., Ltd (Shanghai, China). Triton X-100 were purchased from BBI Life Sciences Co., Ltd. (Shanghai, China). Sodium hydroxide (NaOH, AR), sodium dihydrogen phosphate (NaH_2PO_4, AR), sodium phosphate dibasic (Na_2HPO_4, AR) and other AR reagents are obtained from Lingfeng Reagent Co., Ltd. (Shanghai, China).

2.2. Measurement methods

The morhology of TiO_2 can be obtained by scanning electronic microscopy (SEM) and nitrogen adsorption and desorption curves, respectively. Fourier transform infrared spectroscopy (FTIR) was performed on a NICOLET IS5 spectrometer (Thermo Fisher Scientific, USA). Zeta potential can imply changes in the charge properties of titanium dioxide surface by Zetasizer Nano ZS90 (Malvern, UK). The element content of titanium dioxide surface was carried by X-ray photo-electron spectroscopy (XPS) on an Axis-Nova instrument (Kratos Analytical, Manchester, UK). UV spectrophotometer is used to test the concentration of pNP and enzyme.

2.3 Experimental method

2.3.2. Preparation of titanium dioxide with different pore structures

Synthesis method[25] of TiO_2 particles: using $TiO_2 \cdot nH_2O$ and potassium carbonate as raw materials, treatment in aqueous solution at 810 °C for 2 h to obtain intermediate $K_2Ti_2O_5$ whiskers. $K_2Ti_2O_5$ was placed in water for ultrasonic dispersion, stirring with 0.5 M hydrochloric acid, then suction filtration, and finally washed with water until neutral. After drying, TiO_2 precursor hydrated $H_2Ti_2O_5$ was obtained. The obtained hydrated $H_2Ti_2O_5$ was calcined in a muffle furnace at 400 °C, 650 °C for 2 h, to obtain TiO_2 particles T400, T650.

2.3.3. Coupling agents modification

Take 1 g of P25 and treat it in an oven at 120 °C for 12 h. Then, the P25 and 1 mmol silane coupling agent APTES were mixed in 50 mL toluene, placed in 70°C oil bath and stirred for 8 h, then centrifuged to remove toluene. Washing the precipitate twice with toluene, acetone and ethanol to get rid of excess coupling agent. Finally, P25 modified by APTES was obtained, named as A-P25. Other coupling agents such as ETS, IPTS, and TTS modify P25 in the same way as above, and are named E-P25, I-P25, T-P25. T400 and T650 modification process are the same as above.

2.3.4. Modified amount of coupling agent

The amount of coupling agents added was 1, 0.8, 0.6, 0.4, 0.2 mmol per gram of TiO_2

, then mixed in 50 mL toluene, and placed in a 70 °C oil stirring for 8 h. The following steps are consistent with the previous section.

2.3.5. Immobilization of *Aspergillus oryzae* lipase

Taking 0.1 g of TiO_2 or modified TiO_2 and add 10 mL AOL with a concentration of 0.25 g/L incubated at 25 °C for 2 h. Then, centrifuging at 4000 ×g to obtain the precipitate, and washing it three times with phosphate buffer (0.05 M, pH 7.5) until no protein was eluted. Immobilized lipase was obtained.

2.3.6. Enzyme activity

1 unit (U) of lipase activity was defined as the amount of lipase that convert 1 μmol of pNPP in 1 min under the test conditions. Lipase activity is determined by adding 1 mL free or immobilized lipase suspension to 3 mL of reactant pNPP (in isopropanol) at a certain concentration to make the final reaction system 5mL. The reaction system was placed in a 50 °C water bath for 20 min. After the reaction, immediately measure the UV absorbance at 420 nm. Finally, the product concentration is obtained according to the relationship between the absorbance value and the product concentration, and the catalytic activity is calculated. The activity was measured three times and average value and standard deviation were determined.

The calculation method of enzyme activity is as follows:

$$\text{Specific activity} = \frac{\text{Lipase activity}}{m_L}$$

$$\text{Relative activity} = \frac{U_I}{U_F} \times 100\%$$

$$\text{Activity recovery} = \frac{U_I \cdot m_L}{U_F \cdot m_I} \times 100\%$$

m_L: quality of lipase added during enzyme activity test, g

U_I: measured activity of immobilized lipase, U

U_F: measured free lipase activity, U

m_I: protein loading of immobilized lipase, g/g

2.2.7. The protein loading assay

Protein concentration is measured by Bradford method[26], the protein loading and protein loading efficiency is calculated by the following Eq:

$$\text{Protein loading} = \frac{C_0 \cdot V_0 - C_1 \cdot V_0}{m}$$

$$\text{Protein loading efficiency} = \frac{C_0 \cdot V_0 - C_1 \cdot V_0}{C_0 \cdot V_0} \times 100\%$$

C_0: Initial protein concentration added before immobilization, mg/mL

C_1: the protein concentration in the system after immobilization, mg/mL

V_0: volume of enzyme solution added during immobilization, mL

m: the quality of the support added during the immobilization, g

2.3.8. The stability assay

The free lipase and the immobilized lipase were treated at 25-70 °C for 5 h, and then the catalytic activity was measured immediately at 50°C to obtain the thermal stability data of lipase. The free lipase and the immobilized lipase were placed in NaOH and HCl solution at pH 4.46-10.21 respectively, treated at 25 °C for 5 h, and then their catalytic activity was immediately measured at 50 °C to obtain the pH stability data of lipase. Store free lipase and immobilized lipase at 4 °C, and measure their catalytic activity every week to get storage stability.

3. RESULTS AND DISCUSSION

3.1 Geometric structure control of TiO_2

We successfully obtained T400, and T650 with different geometric structures by

controlling the calcination temperature of TiO_2. In order to investigate the effect of geometric structure, such as morphology, surface area and pore size on the lipase adsorption and catalytic performance, P25 was selected as the counterpart. Figure 1A shows the the N_2 adsorption/desorption isotherm curves of P25, T400 and T650. All three types of TiO_2 exhibit typical IV adsorption isotherms, indicating the existence of mesopores. The hysteresis loops appear in T400 and T650 indicate that they have a good pore structure.

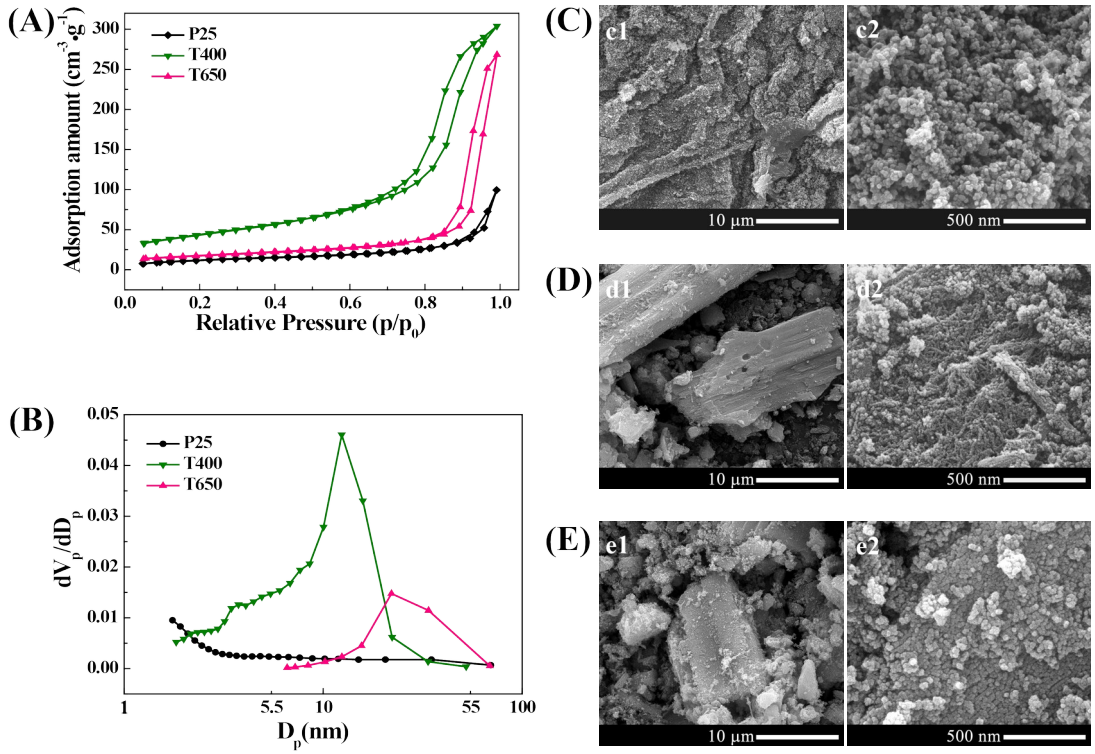

FIGURE 1 N_2 adsorption/desorption isotherm curves (A) and pore size distribution curves (B) of TiO_2 at different calcination temperatures; SEM images of P25 (C), T400 (D), T650 (E) at different resolutions.

Specific surface area and pore volume calculated according to the BJH method are listed in table S1. The pore size distribution diagram (Figure 1B) shows T400 and T650 have narrow pore size distribution, with the mean pore sizes being 11.6 nm and 21.1 nm, respectively. P25 is a non-porous small particle as shown in Scheme 1, and has almost the same specific surface area as T650. In addition to the N_2

adsorption/desorption isotherm curves, we also observed The morphology of the TiO_2 surface was investigated by using SEM.

Figrue 1C shows P25 is an agglomerate composed of non-porous spherical nanoparticles around 50 nm. Both T400 and T650 have mesoporous structure, and T650 with a higher calcination temperature has a larger pore size.

3.2 Surface modification of TiO_2 by coupling agents

The surface properties of TiO_2 are regulated on the basis of the geometric structure. APTES, ETS, IPTS, TTS were used to modify P25, T400, T650, respectively. Take P25 as a representative to compare whether modified by the coupling agents has an effect on the surface morphology. P25 shows a similar surface morphology after the modification by the coupling agents according to the TEM images (Figure S1A).

Through the comparison of the FTIR spectra of Figure 2A and 2B, the grafting of coupling agents were confirmed. In Figure 2A, the broad and large peak at 3415 cm^{-1} indicates the superposition of Ti-OH stretching vibration and -OH of physically adsorbed water on the P25 surface.[27] A large number of hydroxyl groups provide binding sites for coupling agents grafting[28]. The sharp decrease of -OH peak at 3425 cm^{-1} implies the successful grafting of the coupling agent with hydroxyl groups on the surface of P25 nanoparticles. The decrease in the number of hydroxyl groups indicates the improved hydrophobicity of P25.[27] The low-intensity peak at 1640 cm^{-1} can be ascribed to the -OH bond of physically adsorbed water.[29] The broad and strong absorption peak at 800-500 cm^{-1} is assigned to the Ti-O-Ti bond.[29] The new peak at 2870-2950 cm^{-1} was assigned to C-H vibration of coupling agent.[30]

The FTIR spectra of P25 modified by APTES, ETS, and IPTS display absorption peaks at 1040 cm^{-1}, which are due to the antisymmetric stretching vibration of Si-O-Si, indicating a condensation reaction has occurred between the coupling agent molecules[30]. The peak of A-P25 at 1518 and 1220cm^{-1} were assigned to the NH_2

bending vibration and C-N vibration.[28] The FTIR absorption peak of E-P25 at 1418 cm^{-1} corresponds to the C=C bond, indicating the grafting of ETS[27]. The peak at 1527 cm^{-1} was attributed to the NHCO groups which is the result of the reaction between OH groups and isocyanate groups (-NCO). The peak at 1390-1460 cm^{-1} were due to the $-CH_2$ of the TTS. These results were clear evidence of the successful grafting of TTS with P25. The peak at 1070-1060 cm^{-1} can be attributed to C-OH or Ti-OH, which was formed during the reaction. The peak at 917 cm^{-1}, corresponding to stretching vibration of Ti-O-Si bond, reconfirmed the condensation reaction between R groups of coupling agents (general formula: $RSiX_3$) and the TiO_2 surface hydroxyl groups. This suggests that the four coupling agents are successfully grafted onto TiO_2 surface through chemical bonds. The spectra of T400 related samples are shown in Figure 2B. It can be seen that the -OH absorption peak at 3425 cm^{-1} of T400 is larger, indicating that T400 has more -OH than the surface of P25. After the modification of the coupling agents, the change of the functional groups on the surface of T400 is consistent with that of P25, but the -OH absorption peak at 3425 cm^{-1} of T400 is still relatively large.

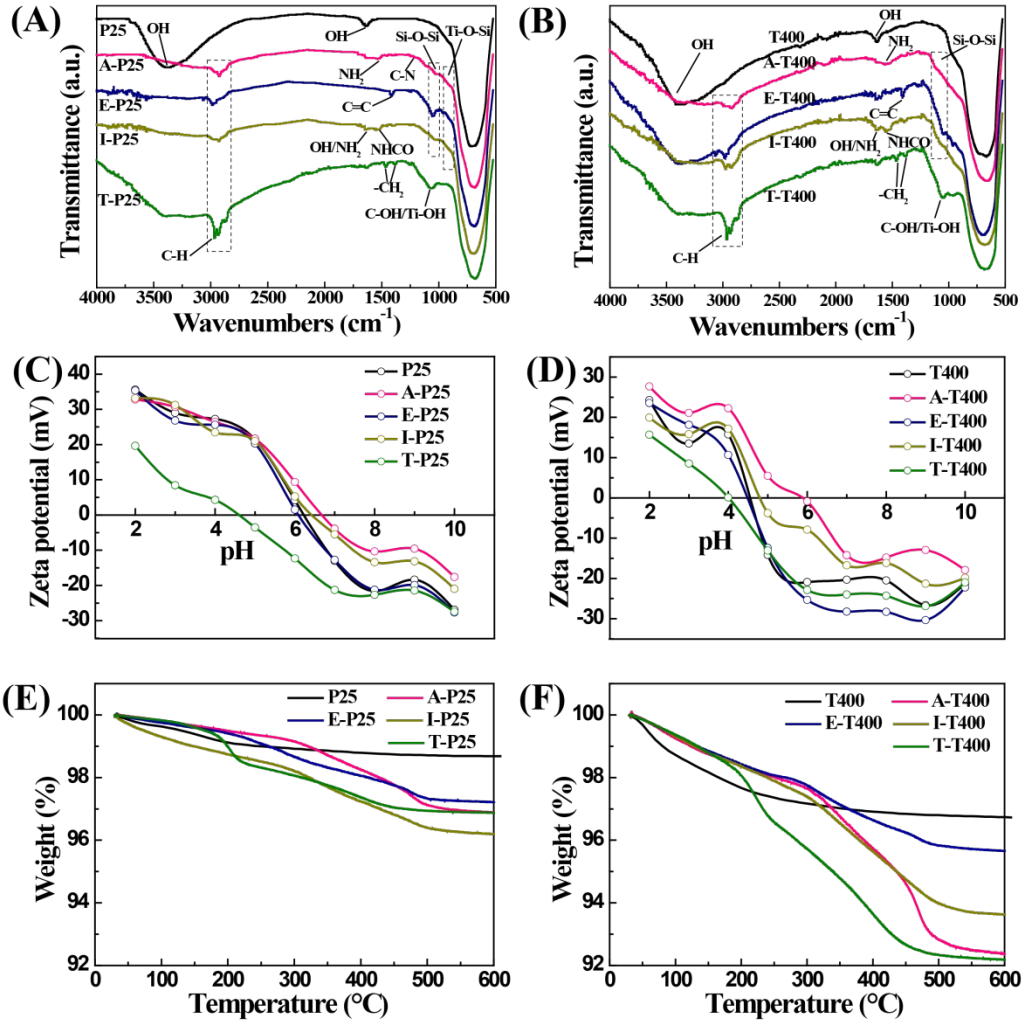

FIGURE 2 FTIR spectra (A, B), Zeta potentials (C, D) and TGA curves (E, F) of original and modified P25 and T400 by different coupling agents.

The Zeta potential image in Figure 2C and 2D showed the change in charge after the coupling agents were grafted. In Figure 2C, the isoelectric point of P25 after TTS modification shifts to the left. TTS produces more acidic groups after reacting with TiO_2 such as titanic acid, resulting in a strong electronegativity of the support. The isoelectric point of E-P25 is very close to that of P25, because ETS does not contain ionizable groups. A small amount of amino groups exposure during the modification of APTS and ITS caused the shift of isoelectric point to the right. The Zeta potential change trends of T400 after coupling agents modification are almost the same as P25. P25 has a higher isoelectric point than T400. This is because T400 has more -OH

connected to Ti because of its high specific surface area, which is consistent with the result of FTIR.

In table S2 is the TG curve. T400 has more weight loss than P25 at 120-800 °C, which is consistent with the results of Zeta potential. The amount of coupling agent molecules grafted or adsorbed on TiO_2 can be seen from the thermal weight loss curve. The amount of coupling agent added in the experiment was 1 mmol/g TiO_2, and the access amounts of coupling agents APTES, ETS, IPTS, and TTS were converted into mass fractions of 22.13 %, 19.03 %, 24.70 %, and 91.50 %, respectively. As shown in Figure 2E and 2F, the weigh lost between 30 °C and 120 °C is due to loss of physically absorbed water. At temperatures from 120 °C to 600 °C, P25 showed no significant weight loss, while P25 modified by other coupling agents all showed different degrees of weightlessness, which corresponds to the decomposition of the coupling agents. According to the weight loss percentage calculated by Figure 2E (table S2) at each temperature stage, the addition of the coupling agent is excessive, and the grafting process is sufficient. In addition, we can also know from table S2 that the grafting amount of the coupling agents of T400 is higher than that of P25, but P25 has the higher amount of grafting per unit area, All of this may be due to the large specific surface area of T400.

XPS was used to analyze the elemental changes of the samples. The XPS Si 2p and N1s spectra of P25 and T400 before and after modification are shown in Figure 3. The appearance of N 1s, Si 2p, C 1s, indicating that the coupling agents were indeed bound to the surface of TiO_2. As shown in Figure 3A, the presence of Si 2p in A-P25, E-P25, and I-P25 proves that APTES, ETS, and IPTS successfully graft on the surface of P25. Because there is no change in state of the Si 2p during the reaction, there is only a single peak. The samples with obvious N1s peaks shown in Figure 3C are A-P25 and I-P25. Other samples contain very little N element due to air. In the N1s spectrum of APTES-modified TiO_2, the peaks for H-N and C-N at 401.25 eV and 399.36 eV come from the $-NH_2$ groups in APTES In IPTS modified TiO_2, the H-N and C-N of N1s at 401.29 eV and 399.57 eV are due to -NH- and $-NH_2$. The binding

energy of N1s modified by IPTS is relatively high, which may be due to the presence of O with strong electronegativity around N.[31] The conclusions of Figure 3B and 3D are consistent with the foregoing. Tables S3 and S4 are the elemental composition of P25 and T400 before and after modification, with C/N greater than 7. If the coupling agent is combined with TiO_2 perfectly, one APTES or IPTS molecule will usually react with three hydroxyl groups of the TiO_2 molecules, that is, three ethoxy groups are removed to form a tripod structure, and the theoretical C/N ratio is 3. If only one ethoxy group reacts with the hydroxyl group of the TiO_2 molecule, the theoretical C/N value should also be 7. In fact, all C/N values are greater than 7, indicating that in addition to grafting through chemical bonds, some coupling agents are adsorbed on the surface of TiO_2 or are connected to the coupling agent that already attached to the surface of TiO_2 through self-polymerization.

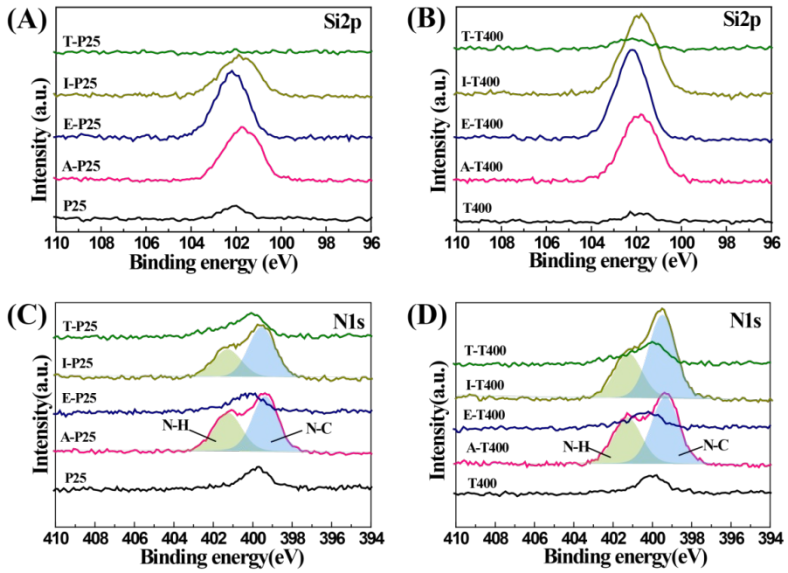

FIGURE 3 High-resolution XPS spectrum of Si 2p and N 1s spectrum of pristine and coupling agents modified P25 (A, C) and T400 (B, D).

3.3 The influence of geometric structure and surface modification on lipase immobilization

Wang *et al.*[32] showed encapsulating catalase on silica nanospheres can also improve its stability, and it still retains 70% of its activity after 25 batches at a wide pH.

Similar observations have also been reported by Pandya *et al*.[4]: α-amylase has higher activity and stability by being immobilized inside the pores.

Figure 4 shows N_2 adsorption/desorption isotherm curves, and the surface area, pore Volume and mean pore size of modified T400 and T650 are shown in Table S5.[4] The pore size distribution of T400, T650, and E-T650 shifted significantly to the left after enzyme immobilization[33], indicating that the enzyme molecules entered the pores. However, the pore size and pore volume of E-T400 did not change significantly after adsorbing the enzyme, indicating that the enzyme did not enter the pore. This is because the surface properties of E-T400 are very suitable for the adsorption of AOL, so it tends to result in the accumulation of enzyme molecules at the entrance of the pore, making it difficult for other enzyme molecules to enter.[17] E-T650 has a larger pore size than E-T400 so that enzymes still enter the pore after modification.

The surface properties of the support, such as pore structure and charge properties, will affect the catalytic properties of the immobilized enzyme. The modification of the coupling agents can regulate the surface properties of TiO_2. Figure 5A and 5B show the influences of pore structure and surface propertie of TiO_2 on the adsorption of AOL. The results of P25 and T650 show that when they have the same specific surface area, the protein loading is higher on the support with pore. T400 has a larger specific surface area than T650, but the protein loading of the two is similar. The research of Bayne et al. showed that as the surface area of enzyme immobilization increases, protein loading will increase sharply at first and then stabilize. Because the reduced pore size on the higher surface area will impair protein loading. However, the activity of T400@AOL is lower than that of T650@AOL, which may be due to the small pore size of T400. The small pore size is likely to cause the substrate replenishment and the product to diffuse slowly. Overall, with the increase of pore size, the protein loading and catalytic activity showed an upward trend.

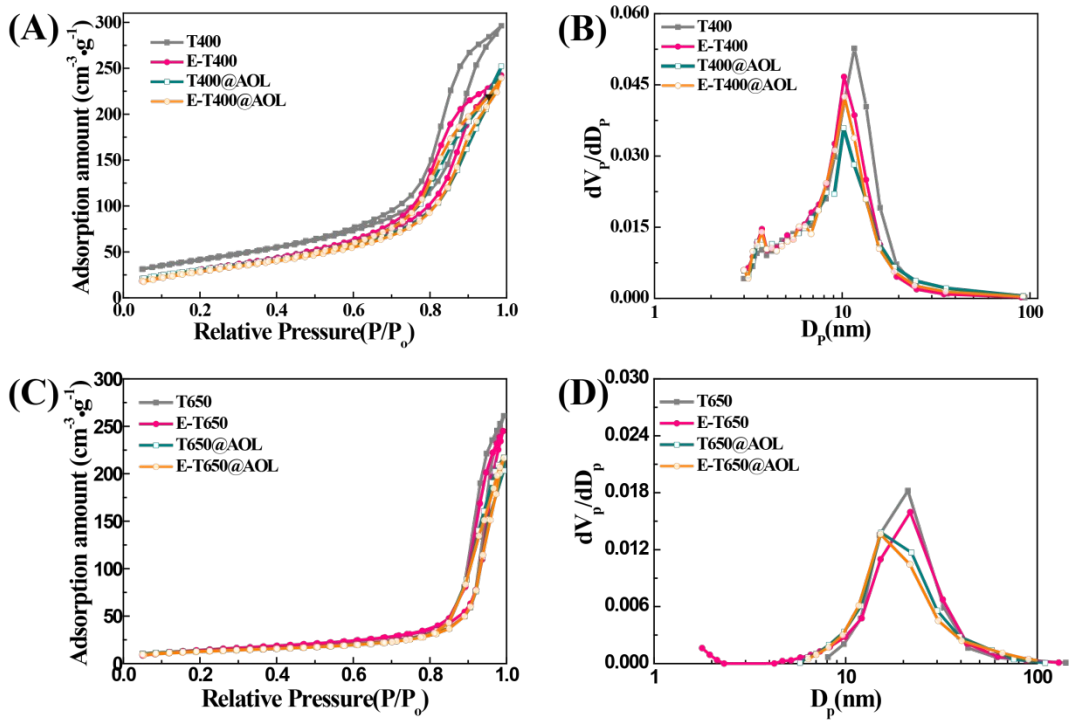

FIGURE 4 N_2 adsorption/desorption isotherm curves (A,C) and pore size distribution (B,D) of T400 and T650 before and after modification and immobilization.

But the pore size has little effect on the catalytic activity and loading of enzyme protein compared with surface properties. The protein loading of coupling agents modified TiO_2 has been improved greatly, and the TiO_2 modified by ETS and TTS has the highest protein loading, especially. It shows that the surface modified by the two coupling agents is the most favorable for the adsorption of AOL. After modification, the chain of the coupling agents will change the pore structure, which will have a complicated effect on the adsorption of lipase. So, the catalytic activity and protein loading of the TiO_2 modified by the same coupling agent immobilized AOL are no longer proportional to the pore diameters. Only TiO_2 modified by ETS has higher catalytic activity than other coupling agents, while the catalytic activity of TiO_2 modified by APTES, IPTS and TTS has not been significantly improved. Among them, E-T650@AOL has the highest relative enzyme activity of 365.85±21.01 %. Since lipase has a hydrophobic lid, the properties of the support surface have a great influence on its catalytic activity[10]. Generally, suitable negatively charged and

hydrophobic supports are more suitable for the adsorption of lipase and the improvement of catalytic activity.

The catalytic activity of E-T650@AOL is higher than E-T400@AOL, because the presence of AOL into the pore structure. Compared with untreated TiO_2, the protein loading and catalytic activity of ETS modified are greatly increased by 20.6, 10.18, 14.07 times. Compared with ETS, TTS has more negative charge, which results a higher protein loading, but its hydrophobicity of TiO_2 has not changed much, so its catalytic activity of immobilized enzyme is still very low.

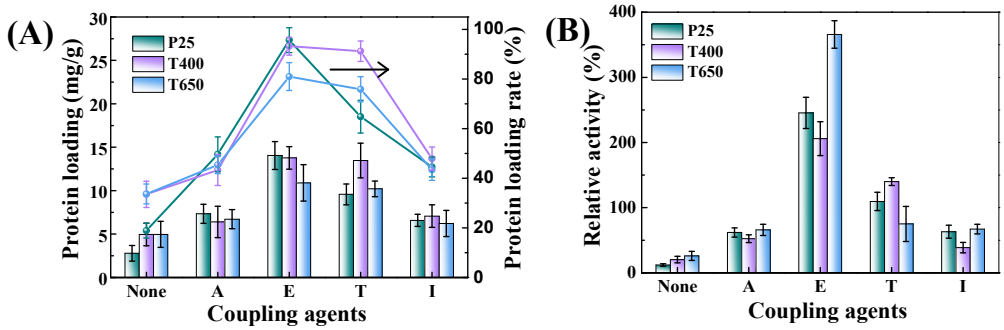

FIGURE 5 Protein loading (A) and catalytic activity (B) of P25, T400 and T650 modified by different coupling agents immobilized lipase.

In order to rule out the lower activity of E-P25 and E-T400 immobilized enzymes than E-T650 is caused by the modification amount of ETS, we optimized the amount of coupling agents ETS for E-P25 and E-T400. As shown in Figure 6A and 6B, the catalytic activity and protein loading of TiO_2 immobilized AOL increase with the addition of ETS. The catalytic activity of modified P25 immobilized AOL tends to be flat when the amount of coupling agent added is 0.4 mmol/g TiO_2. Due to the small specific surface area of P25, the modification amount of ETS quickly reaches saturation. The high surface area of T400 shows an upward trend at the stage of 0.2-0.8 mmol/g TiO_2 coupling agent dosage. The optimal modification amount of ETS for P25 and T400 is 0.8 mmol/g TiO_2. We also used XPS to analyze the coupling agent grafting dosages. It can be seen from the Si 2p of Figure 6C and 6D that the peak intensity continues to increase with the increase of ETS amount. The binding energy

of Si 2p gradually increases due to the increase in the amount of ETS grafted on the TiO_2.

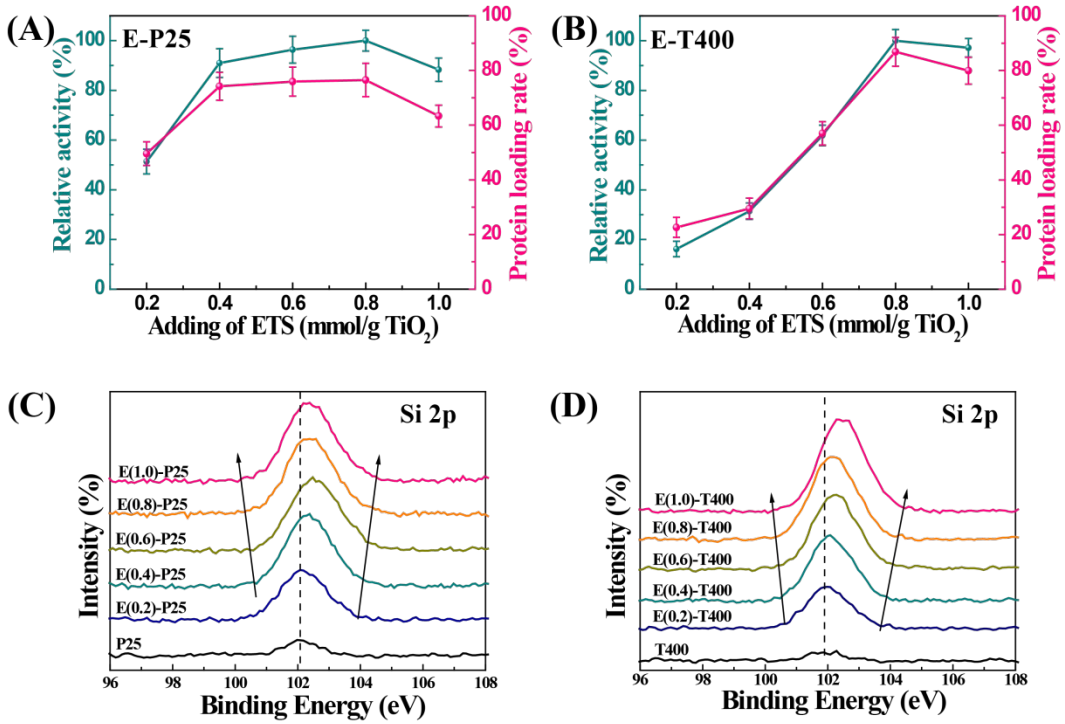

FIGURE 6 Effect of the amount of ETS on the catalytic performance of P25 (A) and T400 (B); Si2p of P25 (C) and T400 (D) under different amounts of ETS.

Figures 7A, B, D show the thermal, pH and storage stability of free AOL and E-P25, E-T400 and E-T650 immobilized AOL, respectively. It can be seen from the Figure 7A E-P25 and E-T400 show excellent thermal stability with the highest activity at 50 °C. AOL and E-T650@AOL obtained their highest activity at 40 °C. This should be due to the higher amount of hydroxyl groups on P25 and T400, which stabilizes the activity of the immobilized enzyme under high-temperature environment.

Above 50 °C, the catalytic activity of E-T650 is slightly lower than that of free AOL. The stability of E-T650@AOL is not improved because the pore is much larger than the size of enzyme molecule, so the enzyme molecule cannot be protected and retained. In the case of physical adsorption, if not encapsulated, enzyme molecules may also leach out of the pores. As shown in Figure 7B, the acid stability of E-T400 and E-T650 has been enhanced, and the alkali stability has a downward trend. The pH

stability of E-P25 is enhanced compared with free AOL for the whole pH range. Under high alkalinity, the support and lipase are both positively charged, and other environmental factors can easily cause the enzyme and support to be weakly bound and easily fall off. As shown in Figure 7C, the activity of the escaped enzyme accounts for nearly 8.1±1.29 %~15.8±1.5 % of the immobilized enzyme (the initial activity) at pH10. This may be the main reason why the immobilized enzyme is unstable in alkaline environment. This is also a common shortcoming of physical adsorption. It is easy to have higher enzyme activity retention, but the binding is often not strong. One way to avoid enzyme leakage is to encapsulate the enzyme in the pores.[37] It can be seen from Figure 7D that the storage stability of the three immobilized enzymes is higher than that of free enzymes, and the relative activity remains higher than 90 % after 8 weeks, especially E-T650@AOL. It shows that the hydroxyl groups and antibacterial of TiO_2 are beneficial to the storage of immobilized lipase. The pore structure can improve the catalytic activity and protect the conformation of the enzyme, but the unencapsulated pore is more likely to cause the enzyme inactivation when in an unstable environment. The coupling agent ETS greatly improves the enzyme activity. The stability of E-TiO_2 immobilized enzyme is still improved under the premise that the relative enzyme activity is significantly improved.

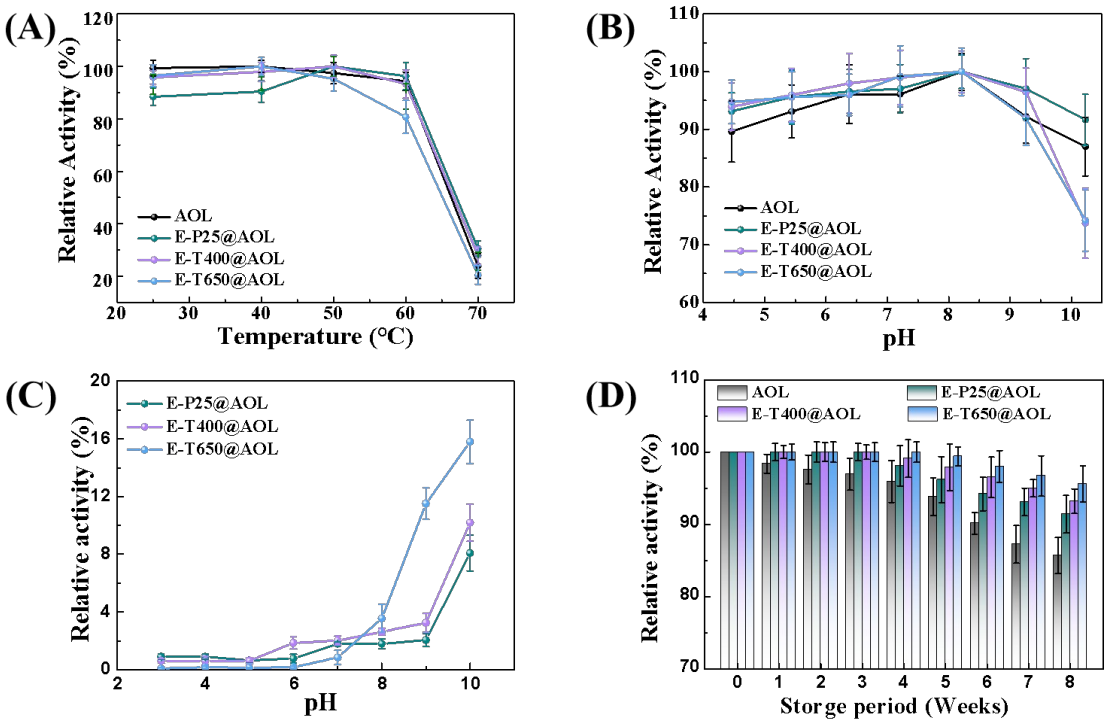

FIGURE 7 Thermal (A), pH (B) and storage (D) stability of free AOL and E-P25, E-T400 and E-T650 immobilized AOL; catalytic activity of part AOL shed from E-P25, E-T400 and E-T650 at different pH (C).

4. CONCLUSIONS

TiO_2 immobilized AOL was used to study the effect of pore size and surface properties on the performance of the immobilized enzyme. P25 and T400 show a huge difference in protein loading, which can be contributed to the difference in pore structure and specific surface area of the supports. The modification of the coupling agents can greatly improve the catalytic performance of the TiO_2-immobilized lipase. ETS-modified TiO_2 shows the greatest improvement in catalytic activity. Therefore, E-T650@AOL with the largest pore size has the highest relative enzyme activity of 365.85 % and excellent storage stability that it retained almost 95% activity after stored at 4 °C for 8 weeks. E-P25@AOL has the greatest improvement of activity, 20.63 times higher than P25@AOL. However, the coupling agents modification

reduces the pore size of support and hinders the entry of enzyme molecules, so the storage stability of E-T400@AOL is lower than that of E-T650@AOL. The pore structure has no significant effect on thermal and pH stability, because the enzyme is prone to leak after deviation from the optimal immobilization conditions for physical adsorption. Our work shows that, compared with the pore structure, the surface properties have a more significant influence on the catalytic performance of the enzyme. Moreover, if the enzyme is only physically adsorbed in the pores, it is still easy to cause enzyme leakage and instability.

Acknowledgements

This work was supported by grants from the National Key Research and Development Program of China (Grant No.: 2019YFD1101204, 2019YFD1101202), the National Natural Science Foundation of China (Grant No.: 21878142, 21776132, 21636003), Key Research and Development Plan of Jiangsu Province (Grant No.: BE2020712), the Jiangsu Synergetic Innovation Center for Advanced Bio-Manufacture, Jiangsu Natural Science Fund for Distinguished Young Scholars (Grant No.: BK20190035), and the Priority Academic Program Development of Jiangsu Higher Education Institutions (PAPD).

References

1. Hanefeld U, Gardossi L, Magner E. Understanding enzyme immobilisation. *Chem Soc Rev.* 2009;38(2):453-468.
2. Mulinari J, Oliveira JV, Hotza D. Lipase immobilization on ceramic supports: an overview on techniques and materials. *Biotechnol Adv.* 2020:107581.
3. Hartmann M, Kostrov X. Immobilization of enzymes on porous silicas–benefits and challenges. *Chem Soc Rev.* 2013;42(15):6277-6289
4. Pandya PH, Jasra RV, Newalkar BL, Bhatt PN. Studies on the activity and stability of immobilized α-amylase in ordered mesoporous silicas. *Micropor Mesopor Mat.* 2005;77(1):67-77.
5. Zhang Y, Zhang J, Huang X, Zhou X, Wu H, Guo S. Assembly of graphene oxide-enzyme conjugates through hydrophobic interaction. *Small.* 2012;8(1):154-159.
6. Adlercreutz P. Immobilisation and application of lipases in organic media. *Chem Soc Rev.* 2013;42(15):6406-6436.
7. Dicosimo R, Mcauliffe J, Poulose AJ, Bohlmann G. Industrial use of immobilized enzymes. *Chem Soc Rev.* 2013;42(15):6437-6474.
8. Rodrigues RC, Virgen-Ortiz JJ, dos Santos JCS. Immobilization of lipases on hydrophobic supports: immobilization mechanism, advantages, problems, and solutions. *Biotechnol Adv.* 2019;37(5):746-770.
9. Zhang DH, Yuwen LX, Li C, Li YQ. Effect of poly(vinyl acetate-acrylamide) microspheres properties and steric hindrance on the immobilization of candida rugosa lipase. *Bioresour Technol.* 2012;124:233-236.
10. Mathesh M, Luan BQ, Akanbi TO. Opening lids-modulation of lipase Immobilization by graphene oxides. *ACS Catal.* 2016;6(7):4760-4768
11. Gao S, Wang Y, Diao X, Luo G, Dai Y. Effect of pore diameter and cross-linking method on the immobilization efficiency of Candida rugosa lipase in SBA-15. *Bioresour Technol.* 2010;101(11):3830-3837.
12. Wei L, Yang B, Chang L. Highly thermal stable and highly crystalline anatase TiO_2 for photocatalysis. *Environ Sci Technol.* 2009;43(14):5423-5428.
13. Wu L, Liu Y, Chi B, et al. An innovative method for immobilizing sucrose isomerase on epsilon-poly-L-lysine modified mesoporous TiO_2. *Food Chem.* 2015;187:182-188.
14. Hao Y, Liu Y, Yang R, Zhang X. A pH-responsive TiO_2-based pickering emulsion system for in situ catalyst recycling. *Chin Chem Lett.* 2018;29:778-782.

15. Qingqing W, Lin P, Guohui L, Ping Z. Activity of laccase immobilized on TiO_2-montmorillonite complexes. *Int J Mol Sci*. 2013;14(6):12520-12532
16. Magner E. Immobilisation of enzymes on mesoporous silicate materials. *Chem Soc Rev*. 2013;42(15):6213-6222.
17. Bayne L, Ulijn RV, Halling PJ. Effect of pore size on the performance of immobilised enzymes. *Chem Soc Rev*. 2013;42(23):9000-9010.
18. Jonkheijm P, Weinrich D, Schroeder H, Niemeyer CM. Chemical strategies for generating protein biochips. *Angew Chem Int Ed*. 2008;47(50):9618-9647.
19. Hartmann M, Jung D. Biocatalysis with enzymes immobilized on mesoporous hosts: the status quo and future trends. *J Mater Chem*. 2010;20(5):844-857.
20. Yang Z, Si S, Zhang C. Study on the activity and stability of urease immobilized onto nanoporous alumina membranes. *Microporous Mesoporous Mater*. 2008;111(1-3):359-366.
21. Zhou Z, Taylor RNK, Kullmann S, Bao H, Hartmann M. Mesoporous organosilicas with large cage-like pores for high efficiency immobilization of enzymes. *Adv Mater*. 2011;23(22-23):2627-2632.
22. Miljkovic MG, Lazic V, Banjanac K, Davidovic SZ. Immobilization of dextransucrase on functionalized TiO_2 supports. *Int J Biol Macromol*. 2018;114:1216-1223.
23. He J, Liu Z, Hai C. Adsorption heterogeneity of lysozyme over functionalized mesoporous silica: effect of interfacial noncovalent interactions. *AlChE J*. 2008;54(9):2495-2506.
24. Wu L, Wu S, Xu Z, Qiu Y. Modified nanoporous titanium dioxide as a novel carrier for enzyme immobilization. *Biosens Bioelectron*. 2016;80:59-66.
25. Zhuang W, Lu L, Wu X, Jin W. TiO2-B nanofibers with high thermal stability as improved anodes for lithium ion batteries. *Electrochem Commun*. 2013;27:124-127.
26. Bradford MM. A rapid and sensitive method for the quantitation of microgram quantities of protein utilizing the principle of protein-dye binding. *Anal Biochem*. 1976;72(1–2):248–254.
27. Ni W, Wu S, Ren Q. Silanized TiO_2 nanoparticles and their application in toner as charge control agents: Preparation and characterization. *Chem Eng J*. 2013;214:272-277.
28. Ponton PI, R.M.d'Almeida J, Marinkovic BA, Savic SM. The effects of the chemical composition of titanate nanotubes and solvent type on 3-aminopropyltriethoxysilane grafting efficiency. *Appl Surf Sci*. 2014;301:315-322.
29. Chen Q, Yakovlev NL. Adsorption and interaction of organosilanes on TiO_2 nanoparticles. *Appl Surf Sci*. 2010;257(5):1395-1400.

30. Ukaji E, Furusawa T, Sato M, Suzuki N. The effect of surface modification with silane coupling agent on suppressing the photo-catalytic activity of fine TiO_2 particles as inorganic UV filter. *Appl Surf Sci.* 2007;254(2):563-569.
31. Sathish M, Viswanathan B, Viswanath RP, Gopinath CS. Synthesis, characterization, electronic structure, and photocatalytic activity of nitrogen-doped TiO_2 nanocatalyst. *Chem Mater.* 2005;17(25):6349-6353.
32. Wang Y, Caruso F. Mesoporous silica spheres as supports for enzyme immobilization and encapsulation. *Chem Mater.* 2005;17:953-961.
33. Lu S, He J, Guo X. Architecture and performance of mesoporous silica-lipase hybrids via non-covalent interfacial adsorption. *AlChE J.* 2010;56(2):506-514.
34. Itoh T, Yano K, Inada Y, Fukushima Y. Stabilization of chlorophyll a in mesoporous silica and its pore size dependence. *J Mater Chem.* 2002;12(11):3275-3277.
35. Vinu A, Murugesan V, Tangermann O, Hartmann M. Adsorption of cytochrome c on mesoporous molecular sieves: Influence of pH, pore diameter, and aluminum incorporation. *Chem Mater.* 2004;16(16):3056-3065.
36. Quiros M, Garcia AB, Montes-Moran MA. Influence of the support surface properties on the protein loading and activity of lipase/mesoporous carbon biocatalysts. *Carbon.* 2011;49(2):406-415.
37. Wang JY, Yu HR, Xie R, Ju XJ. Alginate/Protamine/Silica Hybrid Capsules with Ultrathin Membranes for Laccase Immobilization. *AlChE J.* 2013;59(2):380-389.